Published in final edited form as:
Circ Res. 2010 January 8; 106(1): 193–202. doi:10.1161/CIRCRESAHA.109.198366.

Monoamine oxidase A mediated enhanced catabolism of norepinephrine contributes to adverse remodeling and pump failure in hearts with pressure overload

Nina Kaludercic, PhD[1,2], **Eiki Takimoto, MD, PhD**[1], **Takahiro Nagayama, PhD**[1], **Ning Feng, MD, PhD**[1], **Edwin W. Lai, PhD**[3], **Djahida Bedja, PhD**[4], **Kevin Chen, PhD**[5], **Kathleen L Gabrielson, DVM**[4], **Randy D Blakely, PhD**[6], **Jean C Shih, PhD**[5,7], **Karel Pacak, MD, PhD**[3], **David A Kass, MD**[1], **Fabio Di Lisa, MD**[2], and **Nazareno Paolocci, MD, PhD**[1,8]

[1]Division of Cardiology, Johns Hopkins Medical Institutions, Baltimore, MD, USA

[2]Department of Biomedical Sciences, University of Padova, Italy

[3]Section on Medical Neuroendocrinology, NICHD, NIH, Bethesda, MD, USA

[4]Department of Comparative Pathobiology, Johns Hopkins Medical Institutions, Baltimore, MD, USA

[5]Department of Pharmacology and Pharmaceutical Sciences, University of Southern California, Los Angeles, USA

[6]Center for Molecular Neuroscience and Pharmacology Department, Vanderbilt University, Nashville, TN

[7]Department of Cell and Neurobiology, Keck School of Medicine, University of Southern California, Los Angeles, USA

[8]Department of Clinical Medicine, University of Perugia, Italy.

Abstract

Rationale—Monoamine oxidases (MAO) are mitochondrial enzymes that catabolize pro-hypertrophic neurotransmitters such as norepinephrine and serotonin, generating hydrogen peroxide. Since excess reactive oxygen species (ROS) and catecholamines are major contributors to the pathophysiology of congestive heart failure, MAO could play an important role in this process.

Objective—Here we investigated the role of MAO-A in maladaptive hypertrophy and heart failure.

Methods and results—We report that MAO-A activity is triggered in isolated neonatal and adult myocytes upon stimulation with NE, followed by increase in cell size, ROS production, and signs of maladaptive hypertrophy. All these *in vitro* changes occur in part independently from α- and β-adrenergic receptor-operated signaling and are inhibited by the specific MAO-A inhibitor clorgyline. In mice with left ventricular (LV) dilation and pump failure due to pressure overload, NE catabolism by MAO-A is increased accompanied by exacerbated oxidative stress. MAO-A inhibition prevents these changes, and also reverses fetal gene re-programming, metalloproteinase and caspase-3 activation as well as myocardial apoptosis. The specific role of MAO-A was further tested in mice expressing a dominant-negative MAO-A (MAO-A^{neo}), which were more protected against pressure overload than their wild type littermates.

Correspondence and reprint request to: Nazareno Paolocci, MD, PhD Division of Cardiology/Ross 858 Johns Hopkins School of Medicine 720 Rutland Avenue Baltimore, MD 21205 Phone: (410) 502 6165 FAX: (410) 502-2558 npaoloc1@jhmi.edu.

Disclosures
None.

Conclusions—In addition to adrenergic receptor-dependent mechanisms, enhanced MAO-A activity coupled with increased intramyocardial NE availability results in increased ROS generation, contributing to maladaptive remodeling and LV dysfunction in hearts subjected to chronic stress.

Keywords

MAO-A; congestive heart failure; oxidative stress; catecholamines; serotonin; NET

Introduction

Hemodynamic overload leads to increased cardiac mass and cardiomyocyte volume associated with characteristic changes in gene and protein expression. This initial compensatory hypertrophy is replaced by progressive structural/functional cardiac remodeling involving alterations in extracellular matrix (ECM) composition, myocardial energetics, Ca^{2+} cycling, and myocyte viability[1-4]. Reactive oxygen species (ROS) contribute to each of these abnormalities[5-10], but relevant sources of ROS remain to be fully defined. This is important, as recent studies suggest that specific targeting of ROS sources provides a more effective therapy for heart remodeling[11].

Monoamine oxidases (MAO) are mitochondrial flavoenzymes which catalyze oxidative deamination of catecholamines (CA) and biogenic amines such as serotonin. During this process they generate hydrogen peroxide (H_2O_2), and thus can potentially be a source of oxidative stress in the heart, particularly under stress conditions. Yet, while the role of MAO in terminating neurotransmitter signaling in the brain is well established[12], little is known about its modulation of cardiac morphology and function. MAO exist in two isoforms, MAO-A and –B, with distinct substrate and inhibitor sensitivity[12]. MAO-A, in particular, is present in the myocardium of several species from humans to rodents[13-15], where it principally catabolizes serotonin, norepinephrine (NE) and epinephrine. All these monoamine neurotransmitters have major functional implications in the heart, especially in the modulation of cardiac inotropy. A role for MAO-A and serotonin in ischemic/reperfused myocardium has been delineated showing that inhibiting MAO-A countermands oxidative stress, neutrophil accumulation and mitochondria-dependent cell death[16]. Yet, the involvement of MAO-A and its impact on neurotransmitter availability in congestive heart failure (CHF) remains poorly defined, though one could speculate that this is the type of setting wherein MAO-A might be chiefly at play. CHF is accompanied by enhanced sympathetic tone[17], excess circulating CA such as NE[18], and increased oxidative stress[19]. In such situations, MAO-A may be up-regulated, generating greater amounts of H_2O_2 thus exacerbating disease progression.

Here, we first determined whether cardiomyocyte (both neonatal and adult) exposure to NE is coupled to augmented MAO-A expression/activity which in turn regulates a hypertrophic response linked to the generation of intracellular ROS. Adrenergic receptor independent signaling was assessed using the MAO substrate tyramine. Second, we hypothesized that persistent hemodynamic stress imposed by *in vivo* pressure overload leads to excess CA (and/or serotonin) presence at the myocyte surface resulting in increased sarcolemmal transport via extraneuronal monoamine transporter[20, 21] (EMT), thus enhancing substrate availability for intramyocyte MAO-A activity. To test this, we subjected mice to transverse aortic constriction (TAC), in absence and presence of the highly selective MAO-A inhibitior clorgyline[22], and in mice expressing a dominant negative MAO-A (MAO-A^{neo}). Here we show that NE triggers ROS and myocyte hypertrophy in part by a MAO-A dependent mechanism *in vitro*. *In vivo*, NE catabolism and ROS production are markedly up-regulated in pressure overloaded hearts and both effects are ameliorated by inhibiting MAO-A activity to suppress cardiac decompensation with pressure-overload.

Methods

Animals

For pharmacological studies, male C57BL/6 mice (n=30, 9-11 weeks old) were used and clorgyline was administered using saline as vehicle (1 mg/kg/day, i.p.). For experiments employing genetically modified mice, MAO-A^{neo} mice and their wild type (WT) littermates in 129/Sv background were used (n=30). The Johns Hopkins University Institutional Animal Care and Use Committee approved all animal experiments.

Statistics

All values are expressed as mean±SEM. Comparison between groups was performed by one-way or two-way ANOVA, followed by a Tukey's post-hoc multiple comparison test. Comparisons between two groups were performed using nonpaired 2-tailed Student's t-test. A value of $p<0.05$ was considered significant.

For detailed methods see Supplemental Material.

Results

Norepinephrine triggers cardiomyocyte maladaptive hypertrophy in a MAO-A dependent manner

We first tested whether externally applied NE (as when released from varicosities into the neuroeffector junctional areas) can enter myocytes, stimulating MAO-A activity and ROS-dependent signaling. Cultured rat neonatal cardiomyocytes were incubated with NE (10 μmol/L, 24 hours) which resulted in cell hypertrophy indexed by increased brain natriuretic peptide (BNP) gene expression and 1.3-fold increase in myocyte area (Figure 1 A-B). This effect was accompanied by a rise in MAO-A gene expression and associated with a markedly increased production of mitochondrial ROS, measured with Mitotracker Red (MTR) (Figure 1C-D). In these same experimental conditions, mitochondrial membrane potential was unchanged (Online Figure IV). Co-incubation with the selective MAO-A inhibitor clorgyline[23] (2 μmol/L) significantly blunted NE-induced ROS production and myocyte hypertrophy (Figure 1A, B and D). Similar inhibition was obtained with 5 μmol/L clorgyline (40-50%, data not shown). To test the contribution of adrenergic receptor signaling, myocytes were incubated with tyramine, a MAO substrate that does not interact with adrenergic receptors yet is also transported into cells via EMT[24]. Myocytes treated with tyramine for 24 hours displayed a marked increase in mitochondrial oxidative stress (Figure 1D) and clorgyline prevented this change. Tyramine also increased myocyte area and BNP gene expression (Figure 1E-F), and nuclear factor of activated T-cells (NFAT3) and NFAT4 (Figure 1G) gene expression, the latter transcription factors implicated in maladaptive hypertrophy[25]. Clorgyline inhibited tyramine-induced hypertrophy and suppressed increases in BNP and NFAT expression induced by either NE or tyramine.

We further tested these effects in adult cultured myocytes isolated from WT and MAO-A^{neo} mice, the latter expressing a dominant negative MAO-A resulting in only 8% of residual MAO-A catalytic activity (Figure 6A). WT myocytes challenged with NE displayed a marked arise in ROS production and this was significantly less in myocytes from MAO-A^{neo} mice (Figure 2A). Likewise, increased cell area from NE exposure in WT myocytes was reduced in those from MAO-A^{neo} hearts (Figure 2B). These data further support the hypothesis that, in addition to adrenergic receptors, MAO-A derived ROS also contribute to NE-induced hypertrophy. The fact that in two different systems (neonatal rat and adult mouse myocytes) clorgyline or the genetic suppression of MAO-A activity produced a nearly equal reduction in ROS production and hypertrophy validates clorgyline as a specific MAO-A inhibitor.

Norepinephrine catabolism is increased in failing (TAC) hearts due to enhanced MAO-A activity

We next tested whether these findings pertained *in vivo*. Mice were subjected to TAC and MAO-A gene expression/activity was examined. As expected[19], TAC increased left ventricle (LV) mass to body weight ratio (+330% vs sham, $p<0.001$), chamber dilation and LV dysfunction, all features of adverse remodeling (Table 1). In these hearts, MAO-A gene expression was 3-fold higher (Figure 3A, upper panel). To test for MAO-A activity, we initially performed *in vitro* activity assays using ^{14}C-labeled serotonin as a substrate. No significant differences were observed after 6 weeks of TAC versus sham-controls (Figure 3A, lower panel). MAO activity was also indexed by H_2O_2 production in tissue homogenates in the presence of substrates. Again, no difference was evident (data not shown). To test whether MAO-A activity was up-regulated *in vivo* as a result of increased substrate availability, we measured cardiac NE and serotonin levels in LV specimens of sham and TAC mice. We also assessed the absolute content of dihydroxyphenylglycol (DHPG) and 5-hydroxyindoleacetic acid (5-HIAA) that are the primary catabolic products of NE and serotonin, respectively, due to reactions catalyzed by MAO-A[26]. Absolute cardiac amount of DHPG was significantly elevated in LV tissue extracts of TAC mice, with a consistent marked decrease in cardiac NE content (Figure 3B). When cardiac DHPG content was normalized to intracardiac NE levels, the DHPG/NE ratio was 4-fold higher in TAC hearts vs shams (Figure 3B). Thus, in TAC hearts NE catabolism is increased. Evidence showing that MAO-A inhibition by clorgyline fully reverted the rise in DHPG and DHPG/NE ratio while rescuing the intracardiac content of NE available for release (Figure 3B) supports the specific involvement of MAO-A in this setting.

We also determined whether serotonin, another elective MAO-A substrate, is equally important in this CHF model. Serotonin levels were unaltered by TAC, and rose only after clorgyline treatment, consistent with MAO-A inhibition (Figure 3C). In stark contrast to DHPG, serotonin catabolism measured by 5-HIAA and 5-HIAA/serotonin ratio was not altered in TAC hearts compared to shams. However, clorgyline significantly reduced 5-HIAA/serotonin ratio after TAC. Together, these data show NE to be the preferred substrate fueling MAO-A activity in this model.

Intriguingly, the protein expression of the neuronal NE transporter (NET) declined with TAC, likely reducing neuronal NE re-uptake. Clorgyline treated TAC mice had normal NET expression (Figure 3D) and higher neuronal NE levels.

MAO-A inhibition prevents LV dilation and dysfunction in TAC hearts

We next examined whether MAO-A inhibition was also effective in blunting maladaptive responses to sustained pressure overload *in vivo*. After 3 weeks of TAC, both saline- and clorgyline-treated hearts developed increased wall thickness, but the latter hearts also had preserved LV function: fractional shortening and ejection fraction (EF) values were indeed similar to those reported for sham-controls (Table 1). This beneficial impact on cardiac structure and function became even more pronounced 6 weeks after TAC. Heart weight to body weight ratio was significantly less in the clorgyline-group (Figure 4B), and end-diastolic and end-systolic dimensions were less and not dissimilar from values seen in sham-operated mice (Table 1, Figure 1A). Cardiac function was also fully preserved. Pressure-volume (PV) analysis was also performed to assess if clorgyline had any effects on basal cardiac function over the same time-course of treatment. We found no differences (Online Figure I).

Maladaptive hypertrophy is typically paralleled by fetal gene reprogramming with increased cardiac expression of atrial natriuretic peptide (ANP), BNP and myosin heavy chain β (β-MHC)[25]. Therefore, we tested whether clorgyline treatment restored the adult phenotype expression.

LV mRNA expression for ANP, BNP and β-MHC increased markedly in TAC hearts (Figure 4C), and clorgyline treatment lowered expression of all genes by 2-fold. Thus, MAO-A inhibition prevents both adverse cardiac structural and gene re-programming in pressure-overloaded hearts.

Oxidative stress, MMP activation and apoptosis are blunted in clorgyline-treated TAC hearts

Altered cardiac tissue redox balance is a hallmark of CHF[6, 10], and MAO-A is a recognized source of ROS in ischemia/reperfusion injury[16, 27]. Yet, whether MAO-A up-regulation contributes to CHF pathophysiology in part via enhanced oxidative stress is unknown. Consistent with previous reports[19], ROS were markedly elevated in myocardium of 6-weeks TAC mice detected by dihydroethidium (DHE) staining (Figure 5A). This burden was significantly reduced by clorgyline. Results were further confirmed by measuring tissue malondialdehyde (MDA), an index of lipid peroxidation. MDA amount in TAC hearts was significantly lowere after MAO-A inhibition (Figure 5B).

Since ROS are among the activators of gelatinases such as metalloproteinases MMP-2 and MMP-9 and MMPs are up-regulated in pressure-overloaded hearts[19], we tested whether this was also suppressed by clorgyline. Activities of both MMP-2 and MMP-9 were up-regulated in TAC hearts, and clorgyline reduced this (Figure 5C). We also tested if myocardial apoptosis was involved in TAC-induced CHF and blunted by clorgyline. Cleaved (activated) caspase-3 (Figure 5D) and the number of apoptotic cells measured by TUNEL assay (Figure 5E) markedly rose after 6 weeks of TAC. Clorgyline significantly blunted these adverse phenomena.

MAO-A^{neo} mice display improved LV function, no chamber dilation and reduced levels of fibrosis after TAC

To further establish the specific involvement of MAO-A in TAC-induced cardiac remodeling, we studied mice lacking enzyme activity due to expression of a dominant negative MAO-A (MAO-A^{neo}). These mice display almost null MAO-A activity (Figure 6A), but have preserved levels and activity of MAO-B (Online Figure II). The cardiac phenotype of these mice had yet to be fully characterized, thus load-independent LV function and hemodynamics were examined using *in vivo* PV relationships. WT and MAO-A^{neo} mice were somewhat different at baseline, with LV systolic pressure, dP/dt_{max}, and dP/dt_{min} all lower in MAO-A^{neo} compared to WT littermates (Table 1). Contractile function assessed by preload recruitable stroke work index was also lower in MAO-A^{neo} mice, so these differences were potentially related to loading changes. However, chamber volume and EF were similar between the two strains. When WT and MAO-A^{neo} mice were subjected to 9-weeks TAC, WT hearts had a greater dilation, with a rightward shift in the PV loop (Figure 6A-B), while LV function became impaired. In contrast, MAO-A^{neo} mice showed a slight leftward shift of the PV relations, with preserved (basal) cardiac volumes, and maintained cardiac function. Consistent with the data obtained in C57BL/6 mice, 129/Sv WT mice also displayed reduced NET protein abundance after CHF. In stark contrast, NET levels in MAO-A^{neo} mice were similar to those reported for sham operated mice (Figure 6C). Compared to WT, MAO-A^{neo} mice subjected to TAC also had less interstitial fibrosis (Figure 6D). Thus, genetic inhibition of MAO-A activity also helped ameliorate structural/functional consequences of chronic pressure overload.

Discussion

Changes in cardiac tissue redox balance participate in myocyte hypertrophy and failure, influencing ECM remodeling, Ca^{2+} handling, and metabolic substrate[6, 10, 28]. Clarification of the important sources of ROS therefore has pathogenetic and therapeutic relevance. In the cytosol, NADPH oxidase, xanthine oxidase and uncoupled nitric oxide synthase are recognized ROS sources[10, 19, 29]. Mitochondria are another major source[30, 31], largely from the respiratory

chain and $p66^{Shc}$ [32], and are known to contribute to ischemia/reperfusion injury[33]. Within mitochondria, the flavoenzyme MAO-A, located in the organelle's outer membrane, is a major ROS generator. MAO-A activity is implicated in serotonin-induced myocyte apoptosis[16] and ischemia/reperfusion injury via a ROS-dependent process involving sphingosine kinase inhibition and accumulation of ceramide[27]. MAO-A derived ROS also appear relevant to serotonin-induced myocyte hypertrophy *in vitro*[34].

In this study, we showed that in addition to serotonin, NE catabolism by MAO-A plays a prominent role in hypertrophy *in vitro* and in its progression towards heart failure *in vivo*. Catecholamines, and NE in particular, are known to contribute to cardiac disease and couple to ROS signaling[35]. Enhanced CA synthesis and release may provide help for adaptation to increased workload; however, since NE is a high affinity substrate for MAO-A[36, 37], this can also serve as a major factor for increased ROS, as supported by our *in vitro* myocyte data. Clorgyline partly prevented this change, while the remaining pro-oxidant/hypertrophic effects were likely due to adrenergic receptor-coupled mechanisms[35]. Furthermore, NE metabolism by MAO-A increased in TAC-mice which was also associated with exacerbated oxidative stress, chamber dilation, and reduced systolic function. Pharmacological inhibition of MAO-A suppressed these changes.

Impairment of NE neuronal re-uptake and concomitant down-regulation of the β-adrenergic system are well documented in human and experimental CHF[38], contributing to the loss of systolic performance in this syndrome. In normal hearts, 92% of the NE released by sympathetic nerves is recaptured by NET, 4% is removed by extraneuronal uptake, and the remaining 4% enters the circulation18. However, NET function declines in CHF39, 40 resulting in NE spill-over and extraneuronal uptake which almost doubles in CHF patients[18]. Also, the balance between vesicular NE sequestration (which represents the “measurable” NE pool) and leakage in the intra-cardiac sympathetic efferent fibers may be altered to favor extraneuronal uptake[41], providing more substrate for MAO-A. The current results showing reduced NET expression in TAC hearts support this hypothesis. Increased ROS generation could stem from intramyocyte and/or intraneuronal MAO-A activity as clorgyline inhibits both. The former is supported by the present findings (e.g. Figures 1, 5A-B) whereas proof of the latter would require studies in isolated sympathetic efferent fibers and/or nerve-muscle preparations. Our data also showed that clorgyline or genetic ablation of MAO-A catalytic activity restored NET expression back to control levels in TAC hearts, consistent with findings that systemic administration of MAO inhibitors increases the number of NET recognition sites[42]. This finding hints at the possibility that MAO-A inhibition may also benefit both NE re-uptake and intraneuronal CA recycle for re-release, thereby reducing requirements for transmitter neosynthesis[20].

Prior evidence for MAO-A involvement in cardiac remodeling derives largely from micro-array analyses, showing changes in gene expression in models such as high-salt diet and myocardial infarction[43]. More recently, the role of MAO-A was explored in pressure overload-induced hypertrophy[44]. In this study, Lairez and colleagues showed a role of enhanced serotonin signaling via the $5\text{-}HT_{2A}$ receptor, and found that while antagonizing $5\text{-}HT_{2A}$ was beneficial, genetic deletion of MAO-A proved detrimental, exacerbating LV thickening and fibrosis. While differences in the models could underlie the apparent contradiction with the present findings, other factors might also contribute – such as the severity of the pressure overload. In the prior study, even the WT mice showed little dilation and preserved function. The authors also used WT as opposed to littermate controls (the latter employed in the current study). The C57BL/6 strain develops more severe responses to TAC, and the benefits of clorgyline, which avoids potential adaptive changes in the MAO-A gene deletion mouse models, supports the opposite response. Though our control mice for the $MAO\text{-}A^{neo}$ studies (129/Sv background) developed less hypertrophy (consistent with prior reports45), there was

still substantial dilation that was ameliorated in mice lacking active MAO-A. Other potential contributors to this discrepancy are difference in functional assessment, with anesthesia-induced cardiodepression in the earlier study, versus conscious data in the current experiments. MAO-A^{neo} mice also had basal elevated intracardiac NE content. It remains to be determined whether myocyte-specific gene deletion would yield the same results. In the earlier study of Lairez and collaborators[44], cardiac levels of CA were not determined whereas serotonin levels were found to be increased at baseline in MAO-A$^{-/-}$ mice, consistent with present findings, and did not change when LV remodeling was already established. The latter is also consistent with our study in showing no alteration of serotonin content in TAC-induced CHF. As expected, in both studies MAO-A inhibition increased serotonin levels in TAC hearts. Thus, considering that increased cardiac serotonin content is concomitant with improved LV function and absence of remodeling after TAC, an actual beneficial effect of serotonin cannot be excluded. It is plausible that serotonin may sustain cardiac contractility[46] during late stage CHF, particularly if a deficit in NE availability persists. In the end, this effect would provide an additional explanation for the beneficial action of MAO-A inhibition.

There are some limitations to this study. We did not test the role of MAO-B and catechol-O-methyl transferase (COMT), both additional monoamine catabolic enzymes. However, prior studies in mice and humans have not shown a major role for MAO-B in NE catabolism[36, 37] and COMT gene expression did not change in our TAC model (data not shown). Future studies with pharmacological and genetic ablation of these enzymes will be required to definitively examine their role. The mechanistic intricacies by which MAO-A inhibition preserves NET expression, and likely function (given clorgyline effects on NE content in shams and TAC hearts), warrants further investigation, but a possible major involvement of oxidative/nitrosative stress seems plausible[47]. Finally, any post-transcriptional and/or post-translational regulation of MAO-A is currently under investigation.

In conclusion, the present data supports MAO-A as an important source of ROS which contributes to maladaptive remodeling and myocardial dysfunction in hearts subjected to hemodynamic stress. The latter likely results in NE-mediated MAO-A activation due to depressed neuronal uptake. Whether inhibited ROS production and improved NE cycling/availability are the only keys to interpret the beneficial impact of MAO-A inhibition in pressure overloaded hearts needs further investigation. However, present findings add MAO-dependent signaling as a cause of stress-induced maladaptive hypertrophy and pump failure. The data also suggest that MAO-A inhibitors may prove useful in other models of cardiac failure. In the past, non-selective MAO inhibition was associated with the so-called “cheese reaction”, consisting of severe hypertensive crises following the ingestion of food rich in tyramine[37]. However, the generation of new MAO-A inhibitors lacking this limiting side-effect makes even more attractive the idea of advancing such therapy for clinical use in CHF patients.

Supplementary Material

Refer to Web version on PubMed Central for supplementary material.

Acknowledgments

We gratefully acknowledge Dr. Graeme Eisenhofer for insightful suggestions and critical revision of the manuscript and Raymond Johnson at Vanderbilt Neuroscience Core for his invaluable help with HPLC assays. We also thank the Ross confocal facility (NIH/R24DK064388, The Hopkins Basic Research Digestive Disease Development Core Center) for confocal microscope access and John Gibas for technical assistance.

Sources of funding

This work has been supported by American Heart Association (Post-Doctoral Grant to NK and SDG to NP), by MIUR and CNR (FDL), by NIH (HL093432 to ET, HL088649 to KLG, HL56693 to RDB, HL-089297 and HL-077180 to

DAK, R01HL075265 and HL091923 to NP) and in part by the Intramural Research Program of the NICHD NIH, by NIMH Grant R37 MH39085 (Merit Award), RO1 MH67968, Boyd and Elsie Welin Professorship Award (to JCS).

Non standard abbreviations and acronyms

5-HIAA	5-hydroxyindoleacetic acid
5-HT	5-hydroxytryptamine
ANP	atrial natriuretic peptide
BNP	brain natriuretic peptide
CA	catecholamines
CHF	congestive heart failure
COMT	catechol-O-methyl transferase
DHE	dihydroethidium
DHPG	dihydroxyphenylglycol
ECM	extracellular matrix
EF	ejection fraction
EMT	extraneuronal monoamine transporter
LV	left ventricle
MAO	monoamine oxidase
MDA	malondialdehyde
βMHC	myosin heavy chain β
MMP	metalloproteinase
MTR	Mitotracker Red
NE	norepinephrine
NET	norepinephrine transporter
PV	pressure-volume
ROS	reactive oxygen species
TAC	transverse aortic constriction

References

1. Spinale FG. Myocardial matrix remodeling and the matrix metalloproteinases: influence on cardiac form and function. Physiol Rev 2007;87:1285–342. [PubMed: 17928585]
2. Taegtmeyer H, Wilson CR, Razeghi P, Sharma S. Metabolic energetics and genetics in the heart. Ann N Y Acad Sci 2005;1047:208–18. [PubMed: 16093498]
3. Kranias EG, Bers DM. Calcium and cardiomyopathies. Subcell Biochem 2007;45:523–37. [PubMed: 18193651]
4. Colucci WS, Sawyer DB, Singh K, Communal C. Adrenergic overload and apoptosis in heart failure: implications for therapy. J Card Fail 2000;6:1–7. [PubMed: 10908092]
5. Gupte SA, Wolin MS. Oxidant and redox signaling in vascular oxygen sensing: implications for systemic and pulmonary hypertension. Antioxid Redox Signal 2008;10:1137–52. [PubMed: 18315496]
6. Takimoto E, Kass DA. Role of oxidative stress in cardiac hypertrophy and remodeling. Hypertension 2007;49:241–8. [PubMed: 17190878]

7. Sawyer DB, Siwik DA, Xiao L, Pimentel DR, Singh K, Colucci WS. Role of oxidative stress in myocardial hypertrophy and failure. J Mol Cell Cardiol 2002;34:379–88. [PubMed: 11991728]
8. Sorescu D, Griendling KK. Reactive oxygen species, mitochondria, and NAD(P)H oxidases in the development and progression of heart failure. Congest Heart Fail 2002;8:132–40. [PubMed: 12045381]
9. Dhalla AK, Hill MF, Singal PK. Role of oxidative stress in transition of hypertrophy to heart failure. J Am Coll Cardiol 1996;28:506–14. [PubMed: 8800132]
10. Giordano FJ. Oxygen, oxidative stress, hypoxia, and heart failure. J Clin Invest 2005;115:500–8. [PubMed: 15765131]
11. Moens AL, Takimoto E, Tocchetti CG, Chakir K, Bedja D, Cormaci G, Ketner EA, Majmudar M, Gabrielson K, Halushka MK, Mitchell JB, Biswal S, Channon KM, Wolin MS, Alp NJ, Paolocci N, Champion HC, Kass DA. Reversal of cardiac hypertrophy and fibrosis from pressure overload by tetrahydrobiopterin: efficacy of recoupling nitric oxide synthase as a therapeutic strategy. Circulation 2008;117:2626–36. [PubMed: 18474817]
12. Youdim MB, Edmondson D, Tipton KF. The therapeutic potential of monoamine oxidase inhibitors. Nat Rev Neurosci 2006;7:295–309. [PubMed: 16552415]
13. Rodriguez MJ, Saura J, Billett EE, Finch CC, Mahy N. Cellular localization of monoamine oxidase A and B in human tissues outside of the central nervous system. Cell Tissue Res 2001;304:215–20. [PubMed: 11396715]
14. Saura J, Kettler R, Da PM, Richards JG. Quantitative enzyme radioautography with 3HRo 41-1049 and 3H-Ro 19-6327 in vitro: localization and abundance of MAO-A and MAO-B in rat CNS, peripheral organs, and human brain. J Neurosci 1992;12:1977–99. [PubMed: 1578281]
15. Lowe MC, Reichenbach DD, Horita A. Extraneuronal monoamine oxidase in rat heart: biochemical characterization and electron microscopic localization. J Pharmacol Exp Ther 1975;194:522–36. [PubMed: 1159629]
16. Bianchi P, Kunduzova O, Masini E, Cambon C, Bani D, Raimondi L, Seguelas MH, Nistri S, Colucci W, Leducq N, Parini A. Oxidative stress by monoamine oxidase mediates receptor-independent cardiomyocyte apoptosis by serotonin and postischemic myocardial injury. Circulation 2005;112:3297–305. [PubMed: 16286591]
17. Ferguson DW, Berg WJ, Sanders JS. Clinical and hemodynamic correlates of sympathetic nerve activity in normal humans and patients with heart failure: evidence from direct microneurographic recordings. J Am Coll Cardiol 1990;16:1125–34. [PubMed: 2229759]
18. Eisenhofer G, Friberg P, Rundqvist B, Quyyumi AA, Lambert G, Kaye DM, Kopin IJ, Goldstein DS, Esler MD. Cardiac sympathetic nerve function in congestive heart failure. Circulation 1996;93:1667–76. [PubMed: 8653872]
19. Takimoto E, Champion HC, Li M, Ren S, Rodriguez ER, Tavazzi B, Lazzarino G, Paolocci N, Gabrielson KL, Wang Y, Kass DA. Oxidant stress from nitric oxide synthase-3 uncoupling stimulates cardiac pathologic remodeling from chronic pressure load. J Clin Invest 2005;115:1221–31. [PubMed: 15841206]
20. Eisenhofer G. The role of neuronal and extraneuronal plasma membrane transporters in the inactivation of peripheral catecholamines. Pharmacol Ther 2001;91:35–62. [PubMed: 11707293]
21. Wright CD, Chen Q, Baye NL, Huang Y, Healy CL, Kasinathan S, O'Connell TD. Nuclear alpha1-adrenergic receptors signal activated ERK localization to caveolae in adult cardiac myocytes. Circ Res 2008;103:992–1000. [PubMed: 18802028]
22. Tipton KF, Boyce S, O'Sullivan J, Davey GP, Healy J. Monoamine oxidases: certainties and uncertainties. Curr Med Chem 2004;11:1965–82. [PubMed: 15279561]
23. Youdim MB, Finberg JP. New directions in monoamine oxidase A and B selective inhibitors and substrates. Biochem Pharmacol 1991;41:155–62. [PubMed: 1989626]
24. Coatrieux C, Sanson M, Negre-Salvayre A, Parini A, Hannun Y, Itohara S, Salvayre R, Auge N. MAO-A-induced mitogenic signaling is mediated by reactive oxygen species, MMP-2, and the sphingolipid pathway. Free Radic Biol Med 2007;43:80–9. [PubMed: 17561096]
25. Frey N, Olson EN. Cardiac hypertrophy: the good, the bad, and the ugly. Annu Rev Physiol 2003;65:45–79. [PubMed: 12524460]

26. Fujii T, Yamazaki T, Akiyama T, Sano S, Mori H. Extraneuronal enzymatic degradation of myocardial interstitial norepinephrine in the ischemic region. Cardiovasc Res 2004;64:125–31. [PubMed: 15364620]
27. Pchejetski D, Kunduzova O, Dayon A, Calise D, Seguelas MH, Leducq N, Seif I, Parini A, Cuvillier O. Oxidative stress-dependent sphingosine kinase-1 inhibition mediates monoamine oxidase A-associated cardiac cell apoptosis. Circ Res 2007;100:41–9. [PubMed: 17158340]
28. Sabri A, Hughie HH, Lucchesi PA. Regulation of hypertrophic and apoptotic signaling pathways by reactive oxygen species in cardiac myocytes. Antioxid Redox Signal 2003;5:731–40. [PubMed: 14588146]
29. Murdoch CE, Zhang M, Cave AC, Shah AM. NADPH oxidase-dependent redox signalling in cardiac hypertrophy, remodelling and failure. Cardiovasc Res 2006;71:208–15. [PubMed: 16631149]
30. Di Lisa F, Kaludercic N, Carpi A, Menabo R, Giorgio M. Mitochondrial pathways for ROS formation and myocardial injury: the relevance of p66(Shc) and monoamine oxidase. Basic Res Cardiol 2009;104:131–9. [PubMed: 19242637]
31. Orrenius S. Reactive oxygen species in mitochondria-mediated cell death. Drug Metab Rev 2007;39:443–55. [PubMed: 17786631]
32. Giorgio M, Migliaccio E, Orsini F, Paolucci D, Moroni M, Contursi C, Pelliccia G, Luzi L, Minucci S, Marcaccio M, Pinton P, Rizzuto R, Bernardi P, Paolucci F, Pelicci PG. Electron transfer between cytochrome c and p66Shc generates reactive oxygen species that trigger mitochondrial apoptosis. Cell 2005;122:221–33. [PubMed: 16051147]
33. Di Lisa F, Bernardi P. Mitochondria and ischemia-reperfusion injury of the heart: fixing a hole. Cardiovasc Res 2006;70:191–9. [PubMed: 16497286]
34. Bianchi P, Pimentel DR, Murphy MP, Colucci WS, Parini A. A new hypertrophic mechanism of serotonin in cardiac myocytes: receptor-independent ROS generation. FASEB J 2005;19:641–3. [PubMed: 15703274]
35. Amin JK, Xiao L, Pimental DR, Pagano PJ, Singh K, Sawyer DB, Colucci WS. Reactive oxygen species mediate alpha-adrenergic receptor-stimulated hypertrophy in adult rat ventricular myocytes. J Mol Cell Cardiol 2001;33:131–9. [PubMed: 11133229]
36. Lenders JW, Eisenhofer G, Abeling NG, Berger W, Murphy DL, Konings CH, Wagemakers LM, Kopin IJ, Karoum F, van Gennip AH, Brunner HG. Specific genetic deficiencies of the A and B isoenzymes of monoamine oxidase are characterized by distinct neurochemical and clinical phenotypes. J Clin Invest 1996;97:1010–9. [PubMed: 8613523]
37. Bortolato M, Chen K, Shih JC. Monoamine oxidase inactivation: from pathophysiology to therapeutics. Adv Drug Deliv Rev 2008;60:1527–33. [PubMed: 18652859]
38. Beau SL, Saffitz JE. Transmural heterogeneity of norepinephrine uptake in failing human hearts. J Am Coll Cardiol 1994;23:579–85. [PubMed: 8113537]
39. Backs J, Haunstetter A, Gerber SH, Metz J, Borst MM, Strasser RH, Kubler W, Haass M. The neuronal norepinephrine transporter in experimental heart failure: evidence for a posttranscriptional downregulation. J Mol Cell Cardiol 2001;33:461–72. [PubMed: 11181015]
40. Liang CS, Fan TH, Sullebarger JT, Sakamoto S. Decreased adrenergic neuronal uptake activity in experimental right heart failure. A chamber-specific contributor to beta-adrenoceptor downregulation. J Clin Invest 1989;84:1267–75. [PubMed: 2551925]
41. Eisenhofer G, Kopin IJ, Goldstein DS. Leaky catecholamine stores: undue waste or a stress response coping mechanism? Ann N Y Acad Sci 2004;1018:224–30. [PubMed: 15240373]
42. Lee CM, Javitch JA, Snyder SH. Recognition sites for norepinephrine uptake: regulation by neurotransmitter. Science 1983;220:626–9. [PubMed: 6301013]
43. Mialet-Perez J, Bianchi P, Kunduzova O, Parini A. New insights on receptor-dependent and monoamine oxidase-dependent effects of serotonin in the heart. J Neural Transm 2007;114:823–7. [PubMed: 17473906]
44. Lairez O, Calise D, Bianchi P, Ordener C, Spreux-Varoquaux O, Guilbeau-Frugier C, Escourrou G, Seif I, Roncalli J, Pizzinat N, Galinier M, Parini A, Mialet-Perez J. Genetic deletion of MAO-A promotes serotonin-dependent ventricular hypertrophy by pressure overload. J Mol Cell Cardiol 2009;46:587–95. [PubMed: 19162038]

45. Barrick CJ, Rojas M, Schoonhoven R, Smyth SS, Threadgill DW. Cardiac response to pressure overload in 129S1/SvImJ and C57BL/6J mice: temporal- and background-dependent development of concentric left ventricular hypertrophy. Am J Physiol Heart Circ Physiol 2007;292:H2119–H2130. [PubMed: 17172276]

46. Kaumann AJ, Levy FO. 5-hydroxytryptamine receptors in the human cardiovascular system. Pharmacol Ther 2006;111:674–706. [PubMed: 16960982]

47. Mao W, Iwai C, Qin F, Liang CS. Norepinephrine induces endoplasmic reticulum stress and downregulation of norepinephrine transporter density in PC12 cells via oxidative stress. Am J Physiol Heart Circ Physiol 2005;288:H2381–H2389. [PubMed: 15626688]

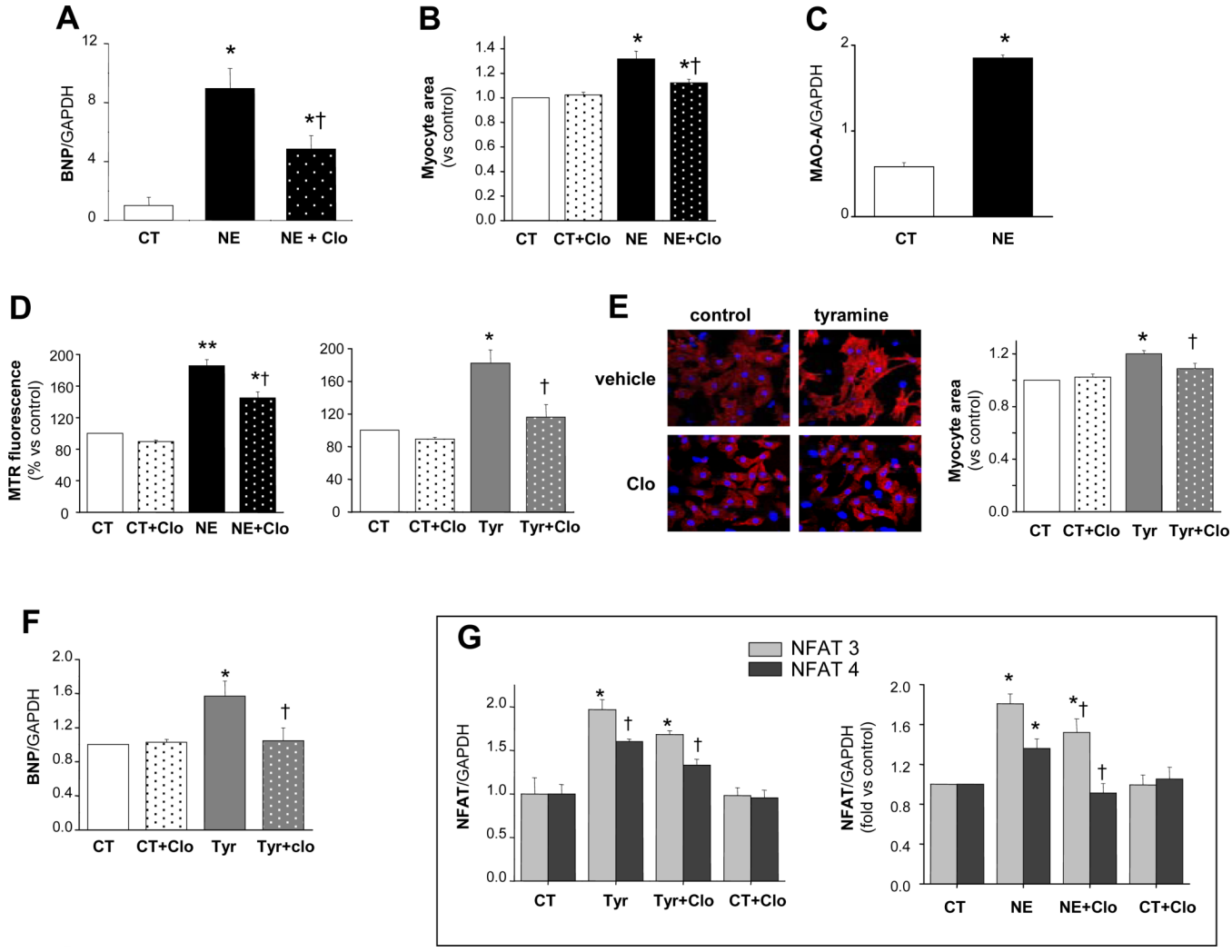

Figure 1.

MAO-A triggers hypertrophy in neonatal rat cardiac myoctes. A: BNP gene expression levels in vehicle- or NE-treated myocytes (10 μmol/L, 24 hrs) in the absence or presence of clorgyline (2 μmol/L). B: Myocyte area measured in control and NE-treated cells (10 μmol/L NE, 24 hours) without or with clorgyline. C: MAO-A gene expression in vehicle and NE-treated cells. D: Mitochondrial ROS production determined by Mitotracker Red after 2 hours of incubation with 10 μmol/L NE (left) or 20 μmol/L tyramine (right), without or with clorgyline. E: Myocyte hypertrophy induced by tyramine determined by α-actinin staining and shown as increase in myocyte area (20 μmol/L, 24 hours). F: BNP gene expression levels in vehicle or tyramine treated myocytes (20 μmol/L, 24 hours), without or with clorgyline. G: NFAT3 and NFAT4 increase in gene expression. *p<0.05 vs control, **p<0.001 vs control, †p<0.05 treatment +clorgyline vs treatment alone.

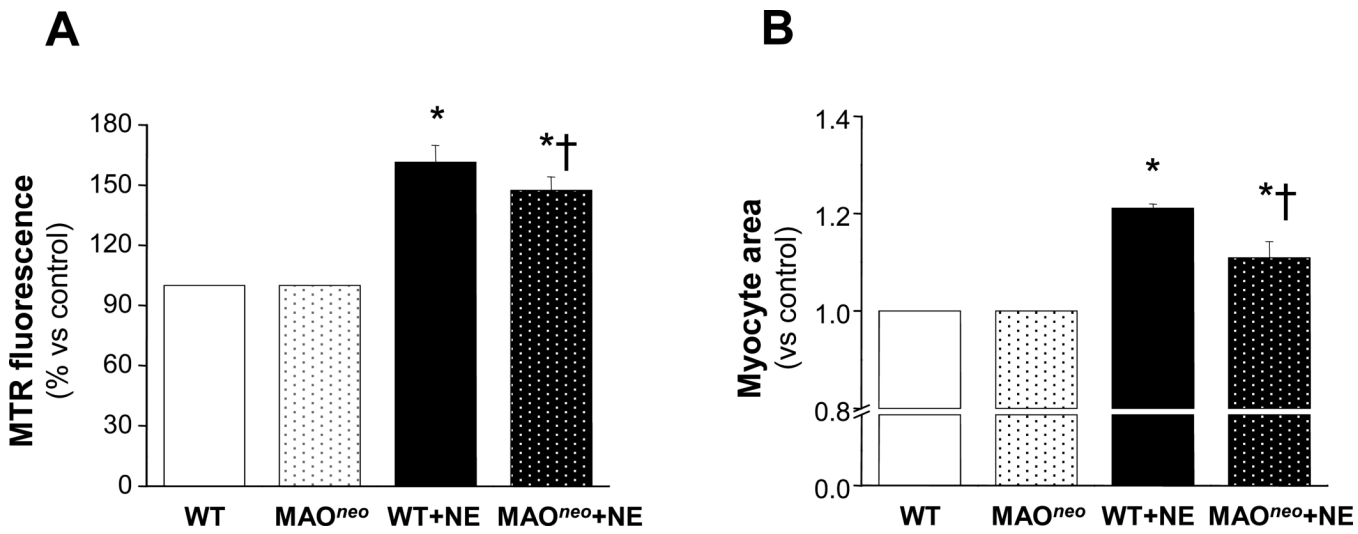

Figure 2.

NE induces ROS formation and hypertrophy in adult mouse ventricular myocytes. A: Mitochondrial ROS production determined by Mitotracker Red after 2 hours of incubation with 10 μmol/L NE in WT and MAO-A^{neo} myocytes. B: Myocyte area measured in WT and MAO-A^{neo} vehicle- and NE-treated myocytes (1 μmol/L NE, 24 hours). *$p<0.001$ vs respective control, $^{\dagger}p<0.005$ vs NE treatment.

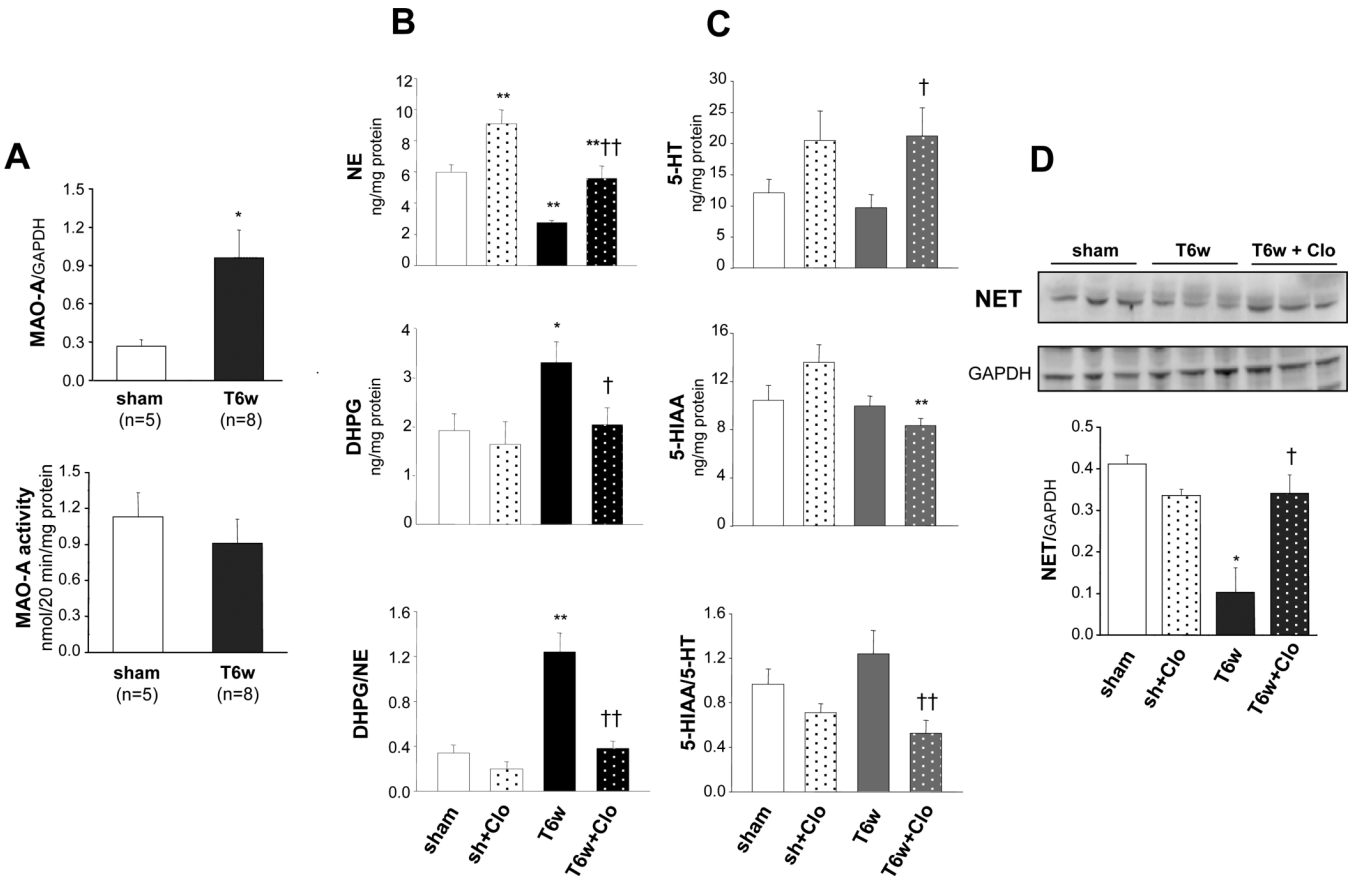

Figure 3.

MAO-A activity and neurotransmitter catabolism is enhanced in pressure overloaded hearts. A: MAO-A gene expression normalized to GAPDH (upper panel) and i*n vitro* MAO-A activity (lower panel) in hearts from sham-operated and 6-weeks TAC mice. B: NE, DHPG content and DHPG/NE ratio in sham and TAC hearts treated without or with clorgyline. C: serotonin (5-HT), 5-HIAA content and 5-HIAA/5-HT ratio in the same groups. D: Western blot for NET and quantification of bands intensity (results normalized to GAPDH expression). T6w: TAC 6 weeks, Clo: clorgyline. *$p<0.05$ vs respective sham, **$p<0.005$ vs respective sham, $^{\dagger}p<0.05$ vs T6w, $^{\dagger\dagger}p<0.005$ vs T6w.

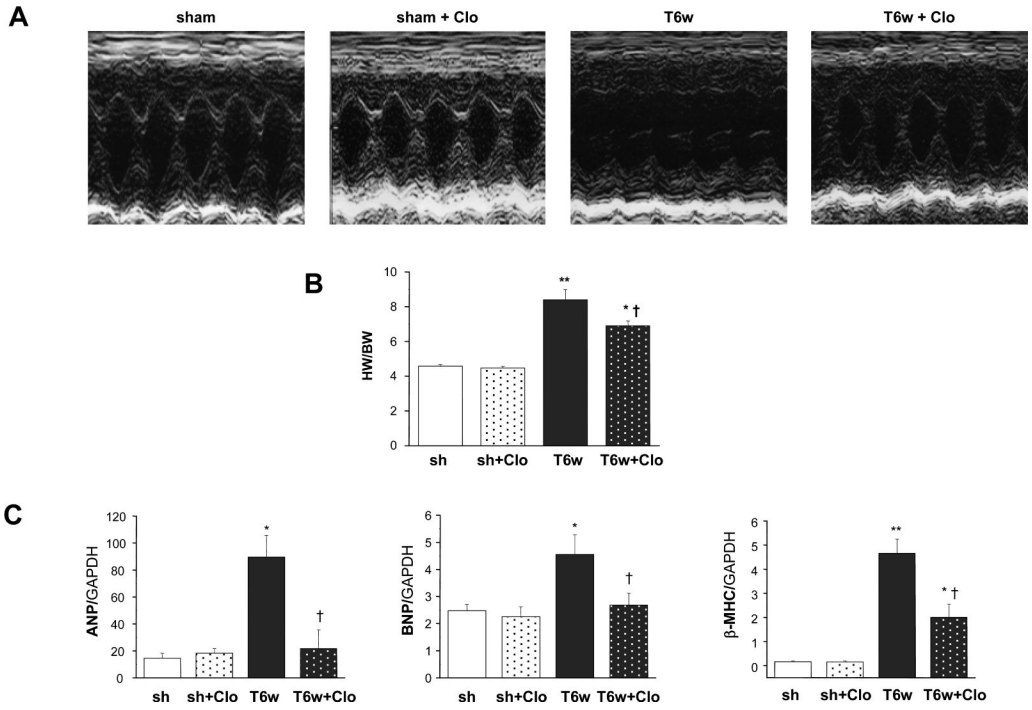

Figure 4.

MAO-A inhibition prevents LV dilation and dysfunction in TAC hearts. A: Representative M-mode echocardiograms, T6w: TAC 6 weeks, Clo: clorgyline. B: Heart weight normalized to body weight (results expressed as mg of heart weight/gram of body weight). D: ANP, BNP and βMHC gene expression. *p<0.05 vs sham, **p<0.001 vs sham, †p<0.05 vs T6w.

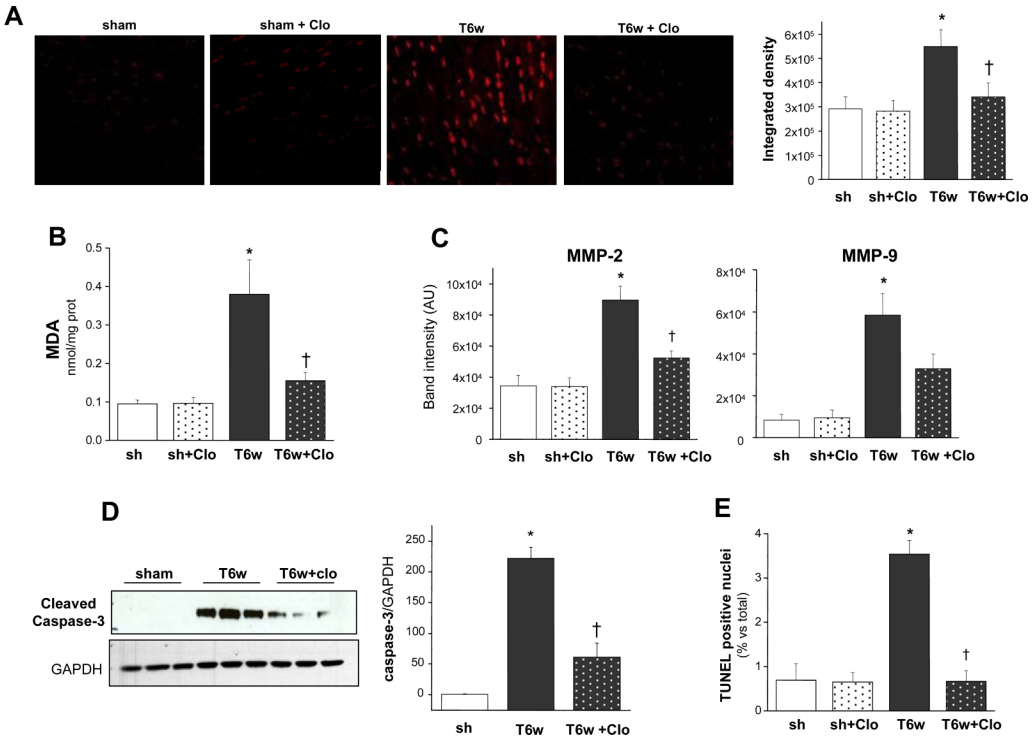

Figure 5.

MAO-A inhibition prevents oxidative stress and apoptosis in pressure overloaded hearts. A: Examples of DHE staining performed on cryosections from sham-operated and 6-weeks TAC hearts without (T6w) or with clorgyline (T6w+Clo). Quantification of DHE fluorescence intensity is shown on the right. B: MDA quantification (results expressed as nmol MDA/mg protein). C: Quantification results of gelatin zymography of myocardium in shams or 6-weeks TAC hearts, without or with clorgyline. D: Western blot showing cleaved (activated) caspase-3 levels (densitometric results on the right). E: Percentage of apoptotic nuclei determined by TUNEL staining versus total number of cells. *$*p<0.05$ vs sham, $^{\dagger}p<0.05$ vs T6w.*

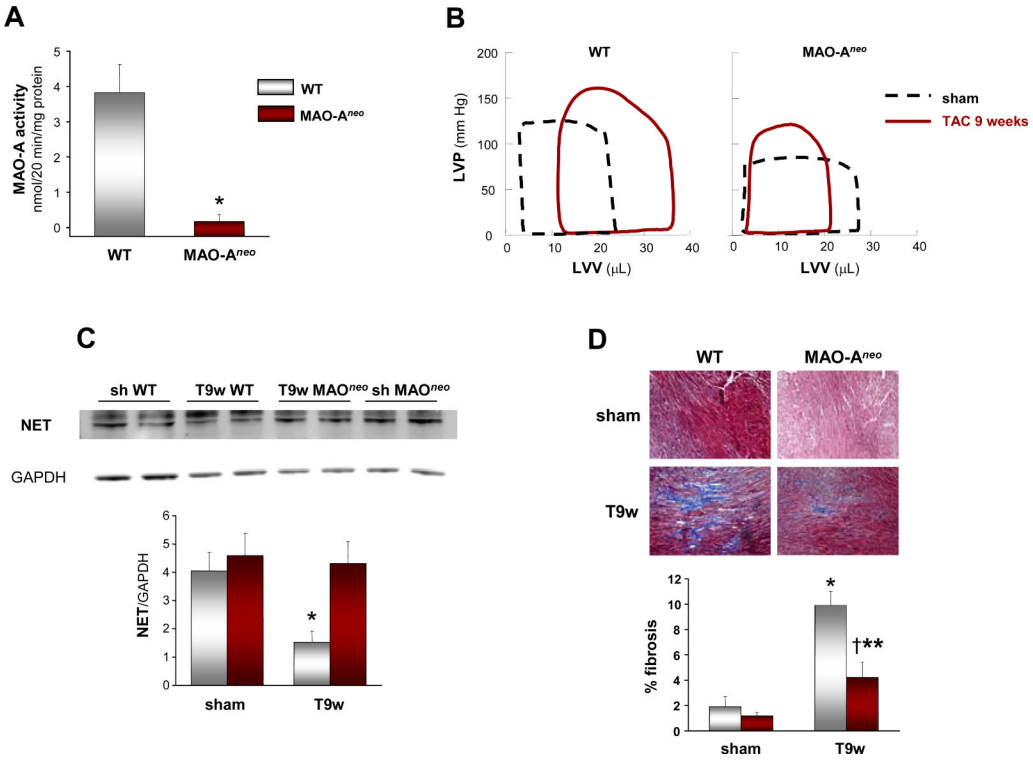

Figure 6.

MAO-A^{neo} mice have preserved LV function and reduced chamber dimensions after pressure overload. A: MAO-A activity in WT and MAO-A^{neo} mice. B: Representative PV loops from WT and MAO-A^{neo} at baseline (dashed line) and 9 weeks after TAC (full line). C: Western blot for NET and quantification of bands intensity (results normalized to GAPDH expression). D: Masson's Trichrome staining of paraffin sections from WT and MAO-A^{neo} mice showing the extent of interstitial fibrosis in shams and 9-weeks TAC hearts (T9w). The quantification of fibrotic areas is shown on the right and results are expressed as percent of myocardial area. *p<0.05 vs WT sham, †p<0.05 vs WT T9w, **p<0.05 vs MAO-A^{neo} sham.

Table 1

Time-dependent changes in cardiac morphology and *in vivo* ventricular function induced by TAC in control and clorgyline-treated mice. IVS: interventricular septum, LVEDD: left ventricular end-diastolic dimension, LVESD: left ventricular end-systolic dimension, LVPW: left ventricular posterior wall, FS: fractional shortening, EF: ejection fraction, BW: body weight, T3w: TAC 3 weeks, T6w: TAC 6 weeks, CLO: clorgyline.

	Sham (n=5)	Sham+CLO (n=5)	T3w (n=8)	T3w+CLO (n=8)	T6w (n=8)	T6w+CLO (n=8)
BW (g)	27.3±0.7	25.7±1.4	25.3±0.6	25.9±0.6	26.6±0.7	27.3±0.3
Heart rate (bpm)	683±21	690±8	674±11	701±11	628±24	665±14
IVS (mm)	0.9±0.02	0.8±0.02	1.3±0.04*	1.2±0.05*	1.2±0.04*	1.3±0.06*
LVEDD (mm)	3.2±0.07	3.2±0.09	2.9±0.2	3±0.1	4±0.2*	3.1±0.08‡
LVESD (mm)	1.3±0.04	1.2±0.06	1.7±0.2	1.3±0.09	2.9±0.4*	1.2±0.05‡
LVPW (mm)	0.8±0.02	0.8±0.03	1.3±0.05*	1.2±0.04*	1.1±0.05*	1.2±0.05*
FS (%)	60.4±0.9	62.7±1.1	43.2±3.5*	56.5±1.9†	30.6±5.3*	61.1±1‡
EF (%)	93.7±0.4	94.7±0.5	80.2±3.6*	91.4±1.1†	62.4±7.9*	94±0.5‡
LV mass/BW	4.3±0.1	4.5±0.05	6.9±0.5*	6.5±0.3*	9.3±0.5*	6.9±0.4*‡

*p<0.05 vs respective sham

†p<0.001 vs TAC 3 weeks

‡p<0.05 vs TAC 6 weeks.

Table 2

Morphological and functional changes via pressure-volume relationships in WT and MAO-A^{neo} mice at baseline and after 9 weeks of TAC (n=5 each group). LVPsys: left ventricular systolic pressure, LVPdia: left ventricular diastolic pressure, LVVes: end-systolic left ventricular volume, LVVed: end-diastolic left ventricular volume, EF: ejection fraction, τ: relaxation constant, PRSW: preload recruitable stroke work.

	genotype	Sham	TAC 9 weeks
Heart rate (bpm)	WT	537±10	503±23
	MAO-A^{neo}	515±28	501±19
Peak LVPsys (mm Hg)	WT	119±6	162±14†
	MAO-A^{neo}	97±6*	137±17†
LVPdia (mm Hg)	WT	1±0.3	2±1
	MAO-A^{neo}	2±1	2±0.7
LVVes (μl)	WT	4.5±1	16.6±4.5‡
	MAO-A^{neo}	5.7±2.4	5.5±1.4§
LVVed (μl)	WT	27.1±2.5	39.4±3.1†
	MAO-A^{neo}	28.1±5	25.7±3.6§
EF (%)	WT	83.8±1.9	59.7±8.3‡
	MAO-A^{neo}	80.6±5.3	79.3±2.6§
dp/dt$_{max}$ (mm Hg/s)	WT	16140±405	13796±226‡
	MAO-A^{neo}	12681±1391*	12963±991
dp/dt$_{min}$ (mm Hg/s)	WT	−11415±595	−10591±425
	MAO-A^{neo}	−8013±948*	−9663±1192
.τ (ms)	WT	5.6±0.2	5.7±0.1
	MAO-A^{neo}	5.9±0.1	5.8±0.5
PRSW (mm Hg)	WT	129.6±8.2	132.3±11
	MAO-A^{neo}	95.3±11.1*	126.2±20.9

*p<0.05 vs WT sham

†p<0.05 TAC vs sham

‡p<0.01 vs WT sham

§p<0.05 vs WT TAC; comparison performed by t-test.